Modulation of Excited-State Intramolecular Proton Transfer Reaction of 1-Hydroxy-2-naphthaldehyde in Different Supramolecular Assemblies

ARTICLE *in* LANGMUIR · MARCH 2010

Impact Factor: 4.46 · DOI: 10.1021/la903196k · Source: PubMed

3 AUTHORS, INCLUDING:

Bijan Kumar Paul
Indian Institute of Science Education and Re…

72 PUBLICATIONS **895** CITATIONS

SEE PROFILE

Langmuir
Article
pubs.acs.org/Langmuir

Modulation of Excited-State Intramolecular Proton Transfer Reaction of 1-Hydroxy-2-naphthaldehyde in Different Supramolecular Assemblies

Bijan Kumar Paul, Anuva Samanta, and Nikhil Guchhait*

Department of Chemistry, University of Calcutta, 92 A. P. C. Road, Calcutta-700009, India

Received August 26, 2009. Revised Manuscript Received November 10, 2009

The excited-state intramolecular proton transfer (ESIPT) reaction of 1-hydroxy-2-naphthaldehyde (HN12) has been studied within the interior of the supramolecular assemblies of α-, β-, and γ-cyclodextrins (CD) and biomimicking environments of ionic (SDS) and non-ionic (TW-20) micelles. Fluorescence measurements are used to investigate the effect of various supramolecular assemblies on the ESIPT reaction by monitoring the large Stokes-shifted tautomer emission of HN12. Enhanced tautomer emission in the microencapsulated state predicts favorable ESIPT reaction in the supramoleuclar assemblies. Benesi−Hildebrand plots have been employed to ascertain that the stoichiometric ratios of the complexes formed between HN12 and CDs are 1:2, 1:1, and 1:1 for α-, β-, and γ-CD, respectively. The binding constants (K_1) and free-energy change (ΔG) for inclusion complexation are also determined from the linearized Benesi−Hildebrand plots. Steady-state fluorescence anisotropy, REES, excitation anisotropy, and fluorescence lifetime measurements are in line with other experimental findings. Differential action of urea on SDS and TW-20-bound probe has also been investigated.

1. Introduction

The past few decades have witnessed the importance of organized assemblies on biological and photophysical processes. The structure and properties of chemical entities entrapped in the molecular assemblies like cyclodextrins (CDs), micelles, reverse micelles, microemulsions, vesicles, and so forth have attracted enormous attention compared to that in pure homogeneous media. The study of inclusion complexes are important in fundamental research since it furnishes valuable information about noncovalent intermolecular forces.[1] Apart from this, research in the field of characterization of inclusion complexes has experienced a splendid evolution because of their potential ability in a diverse range of applications. These inclusion complexes can serve as miniature models for studying the mode of action of enzymes,[2,3] mimicking the reactions in biosystems,[3] and so forth. These have promising prospects in future applications like drug delivery,[4] nanometer-sized electronic devices,[5] and development of energy storage devices.[6] Furthermore, inclusion complexes generally give rise to beneficial modifications of guest molecules in terms of solubility enhancement, protection of labile compounds, control of volatility, and so on. In addition, these are used in industry and laboratories as ion-exchangers, as catalyst in chemical reactions or the microencapsulation of sensitive, active, and aromatic substances.[7] The most important property of an inclusion complex is that a "host" component can admit a "guest" component into its cavity without forming any covalent bond.[1,8,9] Cyclodextrins (CDs) are ideal hosts for studying such inclusion complexes. CDs are cyclic molecules composed of elementary glucopyranose units possessing a hydrophobic cavity[1,8,9] of varying size, and they occupy a position of vital importance in supramolecular chemistry. The supramolecular entity formed as a result of encapsulation of appropriately sized molecules into the CD cavity can serve as an excellent miniature model for enzyme−substrate complexes.[3] Similarly, another significant aspect of supramolecular chemistry finds its association with surfactant molecules, which are capable of forming a unique structure known as a micelle. The ability of micelles to mimic the membranes of biosystems in a much simpler model[10−13] has made them an active topic of research in recent years. Surfactant molecules have significant applications in photography, laser science, pharmaceutical chemistry, and so forth, and they can also act as solubility enhancers for a wide range of organic molecules.[13−15]

Although approximately five decades have passed since the first observation of excited-state intramolecular proton transfer (ESIPT) in methyl salicylate (MS) in 1956 by Weller,[16] the importance of the phenomenon crops up even today given the promising roles of various ESIPT molecules in a vast range of applications, such as development of photostabilizers,[17] proton transfer lasers,[18,19] information storage devices at the molecular level,[17,19] and white-light emitting diode,[20] to mention a few. Such

*Corresponding author. E-mail address: nguchhait@yahoo.com (N. Guchhait).

(1) Rekharsky, M. V.; Inoue, Y. *Chem. Rev.* **1998**, *98*, 1875.
(2) Saenger, W. *Angew. Chem., Int. Ed. Engl.* **1980**, *19*, 344.
(3) Villalonga, R.; Cao, R.; Fragoso, A. *Chem. Rev.* **2007**, *107*, 3088.
(4) Ukeama, K.; Hirayama, F.; Irie, T. *Chem. Rev.* **1998**, *98*, 2045.
(5) Xia, Y.; Rodgers, J.; Paul, K. E.; Whitesides, G. M. *Chem. Rev.* **1999**, *99*, 1823.
(6) Hashimoto, S.; Thomas, J. K. *J. Am. Chem. Soc.* **1985**, *107*, 4655.
(7) Mitra, S.; Das, R.; Mukherjee, S. *J. Phys. Chem. B* **1998**, *102*, 3730.
(8) Szejtli, J. *Cyclodextrin Technology*; Kluwer Academic Publisher: Boston, 1988.
(9) Hapiot, F.; Tilloy, S.; Monflier, E. *Chem. Rev.* **2006**, *106*, 767.
(10) Voskuhl, J.; Ravoo, B. J. *Chem. Soc. Rev.* **2008**, *38*, 495.
(11) Respondek, M.; Madl, T.; Gobl, C.; Golser, R.; Zangger, K. *J. Am. Chem. Soc.* **2007**, *129*, 5228.
(12) Mahata, A.; Sarkar, D.; Bose, D.; Ghosh, D.; Girigoswami, A.; Das, P.; Chattopadhyay, N. *J. Phys. Chem. B* **2009**, *113*, 7517.
(13) (a) Singh, R. B.; Mahanta, S.; Guchhait, N. *J. Photochem. Photobiol. B* **2008**, *91*, 1. (b) Singh, R. B.; Mahanta, S.; Guchhait, N. *Chem. Phys. Lett.* **2008**, *463*, 183.
(14) Banerjee, P.; Pramanik, S.; Sarkar, A.; Bhattracharya, S. C. *J. Phys. Chem. B* **2008**, *112*, 7211.
(15) Bhattacharyya, K. *Acc. Chem. Res.* **2003**, *36*, 95 and references therein.
(16) (a) Weller, A. H. *Prog. React. Kinet.* **1961**, *1*, 187. (b) Beens, H.; Grellmann, K. H.; Gurr, M.; Weller, A. H. *Discuss. Faraday Soc.* **1965**, *39*, 183.
(17) Sobolewski, A. L.; Domcke, W. *Phys. Chem. Chem. Phys.* **2006**, *8*, 3410.
(18) Chou, P. T.; Martinez, M. L.; Clements, J. H. *Chem. Phys. Lett.* **1993**, *204*, 395.
(19) (a) Chou, P. T.; MxMorrow, D.; Aartsna, T. J.; Kasha, M. *J. Phys. Chem.* **1984**, *88*, 4596. (b) Park, S.; Kown, O.-H.; Kim, S.; Park, S.; Choi, M.-G.; Cha, M.; Park, S. Y.; Jang, D.-J. *J. Am. Chem. Soc.* **2005**, *127*, 10070.
(20) Service, R. F. *Science* **2005**, *310*, 1762.

a colossal impact of the phenomenon of ESIPT in applied research has eventually led this phenomenon to become an indispensable building block of photochemistry. Quite a number of works have reported on the study of intramolecular charge transfer (ICT)[21−27] and intermolecular excited-state proton transfer (ESPT)[28,29] reactions in inclusion complexes of CDs and micellar environments. However, reports casting light on the interaction of ESIPT molecular framework with CDs and micelles are comparatively fewer.[7,30,31] Roberts et al. studied the photophysics of 2-(2′-hydroxyphenyl)benzimidazole (HBI) in cyclodextrins and various solvents. They showed the weak intramolecular hydrogen bonding in HBI and formation of strong intermolecular hydrogen bonds with various cyclodextrins and solvent molecules.[31] Hansen et al. demonstrated enhancement of PT reaction of 1-aminopyrene in β-CD cavity.[32] Similarly, Chattopadhyay pointed out that excited-state proton transfer is dependent not only on the microenvironment of the molecule, but also upon the nature of the compound itself.[33]

The photophysical properties of a potent ESIPT molecule, viz., HN12, have been investigated in detail by Singh et al.[34] In this paper, we investigate the modulation of photophysics of HN12 upon formation of inclusion complexes with α-, β-, and γ-CDs and upon interacting with different surfactant molecules in aqueous medium. This study is an attempt to unravel the properties of these assemblies utilizing ESIPT reaction of a potent fluorescent molecule HN12. The present work explores the efficiency HN12 as a potential fluorescence probe for understanding its interaction with relevant biomimicking and supramolecular entities.[13]

2. Experimental Section

2.1. Synthesis and Materials. The synthesis and purification of the compound HN12 has been described elsewhere.[34] Triply distilled deionized water was used throughout the study. Sodium hydroxide (NaOH) and sulfuric acid (H_2SO_4) from E-Merck was used as supplied. α-, β-, and γ-Cyclodextrins from Sigma (Aldrich), USA, and SDS and TW-20 from Qualigen, India, were used as supplied. Urea from Qualigen, India, was used after proper recrystallization from methanol.

2.2. Instruments and Methods. The absorption and emission measurements were done by Hitachi UV−vis U-3501 spectrophotometer and Perkin-Elmer LS-50B fluorimeter, respectively. The concentration of HN12 in all measurements was maintained in the order $(1-1.5)\times10^{-6}$ dm^3-mol^{-1} in order to avoid aggregation and reabsorption effects. In the course of monitoring the influence of cyclodextrin and micellar media on the spectral properties of HN12, a similar set of solutions containing the CDs and surfactants in the absence of the probe (HN12) have been used as blank.

Fluorescence lifetimes were obtained from a time-correlated single photon counting (TCSPC) spectrometer using nanoLED-07 (IBH, U.K.) as the light source at 375 nm to trigger the fluorescence of HN12.[26,27,34] The observed fluorescence intensities were fitted by using a nonlinear least-squares fitting procedure to a function $\left[X(t)=\int_0^t E(t')\ R(t-t')\ \mathrm{d}t\right]$ comprising the convolution of the IRF ($E(t)$) with a sum of exponentials $\left[R(t)=A+\sum_{i=1}^{N}B_i\ \mathrm{e}^{t/\tau_i}\right]$ with pre-exponential factors (B_i), characteristic lifetime (τ_i), and a background (A). The relative contribution of each component was obtained from a triexponential fitting finally was expressed by the following equation:

$$a_n=\frac{B_n}{\sum_{i=1}^{N}B_i}$$

The mean fluorescence lifetimes for the decay curves were calculated from the decay times and the relative contribution of the components using the following equation:

$$\langle\tau_f\rangle=\frac{\sum_i a_i\tau_i^2}{\sum_i a_i\tau_i} \quad (1)$$

Fluorescence quantum yield (Φ_f) was determined using anthracene ($\lambda_{abs}\approx350$ nm and $\Phi_f=0.27$ in MeOH) as the secondary standard in the following equation:

$$\frac{\Phi_S}{\Phi_R}=\frac{A_S}{A_R}\times\frac{(\mathrm{Abs})_R}{(\mathrm{Abs})_S}\times\frac{n_S^2}{n_R^2} \quad (2)$$

where Φ is quantum yield, Abs is absorbance, A is area under the fluorescence curve, and n is the refractive index of the medium. Subscripts S and R denote the corresponding parameters for the sample and reference, respectively.

The steady-state anisotropy is defined as

$$r=\frac{(I_{VV}-G\cdot I_{VH})}{(I_{VV}+2G\cdot I_{VH})} \quad (3)$$

$$G=\frac{I_{HV}}{I_{HH}} \quad (4)$$

in which I_{VV} and I_{VH} are the emission intensities when the excitation polarizer is vertically oriented and the emission polarizer is oriented vertically and horizontally, respectively. G is the correction factor. Steady-state fluorescence anisotropy was measured by Perkin-Elmer LS-50B fluorimeter.

All experiments have been carried out at ambient temperature of 27 °C with air-equilibrated solutions. Only freshly prepared solutions were used for spectroscopic measurements.

3. Results and Discussion

3.1. Steady-State Spectra of HN12 in Pure Homogeneous Fluid. The photophysical properties of HN12 have been reported in detail elsewhere.[34] In brief, the molecule HN12 exhibits absorption bands at ~300, ~375, and ~428 nm in aqueous medium, which are assigned to the neutral/unsolvated open conformer (**II**), intramolecularly H-bonded closed conformer (**I**), and intermolecularly H-bonded solvated complex (**III**), respectively (Scheme 1). The intramolecularly H-bonded closed conformer (**I**) is found to be the lowest energy conformer of HN12 in the ground state.

Upon photoexcitation, the lowest energy closed conformer (**I**) undergoes rapid ESIPT with the signature of large Stokes-shifted emission at ~488 nm attributable to the phototautomer

(21) Krishnamoorthy, G.; Dogra, S. K. *J. Phys. Chem. A* **2000**, 2542.
(22) Hamaski, K.; Iyeda, H.; Nakamura, A.; Uemo, A.; Toda, F.; Suzuki, T.; Osa, T. *J. Am. Chem. Soc.* **1993**, *115*, 5053.
(23) Hazra, P.; Chakrabarty, D.; Sarkar, N. *Langmuir* **2002**, *18*, 7872.
(24) Panja, S.; Chowdhury, P.; Chakravorti, S. *Chem. Phys. Lett.* **2004**, *393*, 409.
(25) Panja, S.; Chakravorti, S. *Chem. Phys. Lett.* **2001**, *336*, 57.
(26) Das, P.; Chakrabarty, A.; Haldar, B.; Mallick, A.; Chattopadhyay, N. *J. Phys. Chem. B* **2007**, *111*, 7401.
(27) Mallick, A.; Haldar, B.; Maiti, S.; Bera, S. C.; Chattopadhyay, N. *J. Phys. Chem. B* **2005**, *109*, 14675.
(28) He, F.; Ramirez, J.; Lebrilla, C. B. *J. Am. Chem. Soc.* **1999**, *121*, 4726.
(29) Hamai, S. *J. Phys. Chem.* **1988**, *92*, 6140.
(30) Roberts, E. L.; Chou, P. T.; Alexander, T. A.; Agbaris, R. A.; Warner, I. M. *J. Phys. Chem.* **1995**, *99*, 5431.
(31) Roberts, E. L.; Dey, J.; Warner, I. M. *J. Phys. Chem. A* **1997**, *101*, 5296.
(32) Hansen, J. E.; Dines, E.; Fleming, G. R. *J. Phys. Chem.* **1992**, *96*, 6904.
(33) Chattopadhyay, N. *J. Photochem. Photobiol. A* **1991**, *58*, 31.
(34) Singh, R. B.; Mahanta, S.; Kar, S.; Guchhait, N. *Chem. Phys.* **2007**, *331*, 373.

Scheme 1. Schematic of the Photophysical Process Observed in HN12

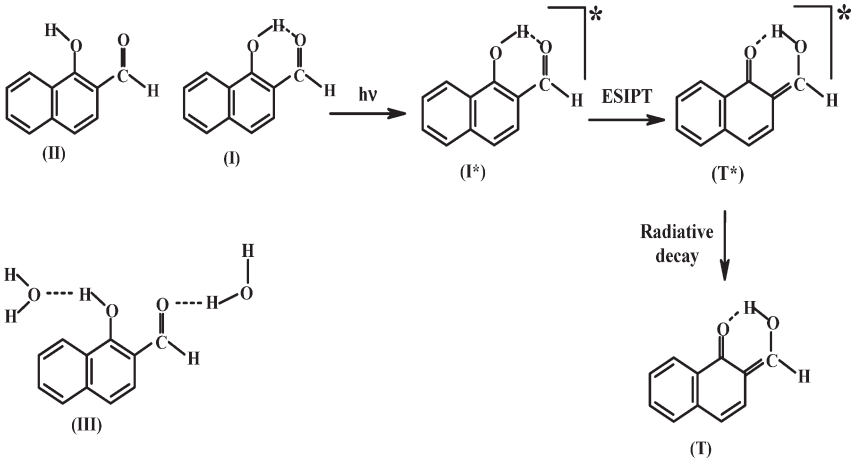

(**T**, Scheme 1). The higher energy emission band at ~353 nm is attributed to an open conformer (**II**) of HN12. Similar ESIPT behavior of HN12 has also been confirmed in other solvents (nonpolar, polar aprotic, and polar protic) too.[34]

3.2. Steady-State Spectra of HN12 in Aqueous Cyclodextrin Medium. The absorption spectra of HN12 in the presence of α-, *β*-, and *γ*-cyclodextrins are displayed in Figure 1 and the variations of absorbance with CD concentration are presented in the insets. The presence of CD is found to introduce no significant shift of the absorption band maxima, but the increment in absorbance is indicative of the formation of the host−guest inclusion complexes. In general, the presence of an equilibrium is indicated by an isosbestic point, but the lack of such an observation during complexation of HN12 with CDs might be due to the strong detergent action of cyclodextrins.[24,25]

Modifications on the emission spectral profile as a result of complexation with CDs are depicted in Figure 2. The insets depict the variation of fluorescence intensity and band maxima positions with increasing CD concentration. Interaction of HN12 with CDs is dramatically reflected on the emission profile through remarkable tautomer emission enhancement and narrowing of the spectra coupled with shifting of the emission maxima toward the blue end of the spectrum with increasing concentration of CDs. It is worth pointing out here that the emission wavelength of HN12 experiences a blue shift upon reduction of medium polarity, e.g., from $\lambda_{em} \sim 488$ nm in aqueous phase to $\lambda_{em} \sim 465$ nm in nonpolar cyclohexane solvent.[34] Therefore, the blue shift in the present case (from $\lambda_{em} \sim 488$ nm to $\lambda_{em} \sim 460$ nm) is argued on the basis of incorporating HN12 into the hydrophobic (nonpolar) interior of CDs.[7,13]

The increment of tautomer emission intensity of HN12 upon complexation with CD may be ascribed to the following reasons: In aqueous medium, the water molecules are not completely excluded from the CD interior during the formation of an inclusion complex. In fact, CDs (particularly *β*-CD) are known to be in a strained configuration due to the presence of water under these conditions.[7,35] This is often cited as one of the driving forces for complexation with hydrophobic species, i.e., to release the strain by driving some of the water molecules out of the CD cavity. Thus, inclusion complex formation with CD results in reduction of the external H-bonding interaction of water molecules with HN12 inside the CD interior, while the intramolecular H-bond in HN12 (**I**, Scheme 1) remains intact. Therefore, solvent perturbation of ESIPT through intermolecular H-bonding interaction[36,37] is minimized in the inclusion complexes of CDs and hence the resultant enhancement of tautomer emission. In addition, one obvious reason for enhancement of tautomer emission is the deactivation of nonradiative decay channels, which operate through intermolecular H-bonds with solvent water molecules.[13,26] However, the increment of fluorescence intensity of HN12 with increasing CD concentration is not linear and begins to level off at a value above ~4−5 mM. These trends could suggest concentrations at which complete complexation is achieved. The spectral changes of HN12 in the presence of *γ*-CD are found to be similar to that with *β*-CD. In the case of α-CD, no spectral change (emission band position or intensity) was observed until [α-CD] = 3 mM and the blue shift of the emission maxima along with intensity increment came into play only above this concentration of α-CD. This result is in accord with the idea that the stoichiometry of the complex formed with α-CD is 2:1 (or higher), since it is only at a reasonably high concentration of α-CD that complexation is set on (stiochiometry of the HN12:CD complexes are discussed in detail in section 2.3).

Hansen et al.[32] studied intermolecular excited-state proton transfer of protonated 1-aminopyrene complexed with *β*-CD, and they found the rate of PT to be enhanced by a factor of 2−3 orders of magnitude relative to that in pure water. On the basis of a spectral blue shift of 1-aminopyrene accompanied by increased fluorescence quantum yield, the H-bonding interaction around the cavity of *β*-CD was inferred to influence the proton transfer rate. Similarly, Chattopadhyay[33] found an increase in the deprotonation rate of carbazole-CD complex and a decrease in that of 2-naphthylamine-CD complex. These data suggest that excited-state proton transfer is dependent not only on the microenvironment of the molecule, but also upon the nature of the compound itself.

The ESIPT reaction in HN12 is found to be ultrafast in nature, and the observed biexponential fluorescence lifetime in water is $\tau_1 = 0.087$ ns ($a_1 = 0.91$) and $\tau_2 = 0.588$ ns ($a_2 = 0.09$) for 488 nm emission.[34] Very similarly, the fluorescence lifetime in cyclohexane is $\tau_1 = 0.722$ ns ($a_1 = 0.91$), $\tau_2 = 1.75$ ns ($a_2 = 0.09$) (the higher lifetime values in aprotic solvents compared to that in polar protic water are attributable to the intermolecular H-bonding assisting nonradiative deactivation[34]). The observed biexponential decay reflects the presence of a major contributing fast component and a slow component with minor contribution. In analogy with the literature data,[7,13,28] the faster component seems attributable to

(35) Szejtli, J. *Chem. Rev.* **1998**, *98*, 1743.

(36) Brucker, G. A.; Kelly, D. F. *J. Phys. Chem.* **1987**, *91*, 2856.
(37) Parthenopoulos, D. A.; Kasha, M. *Chem. Phys. Lett.* **1990**, *173*, 303.

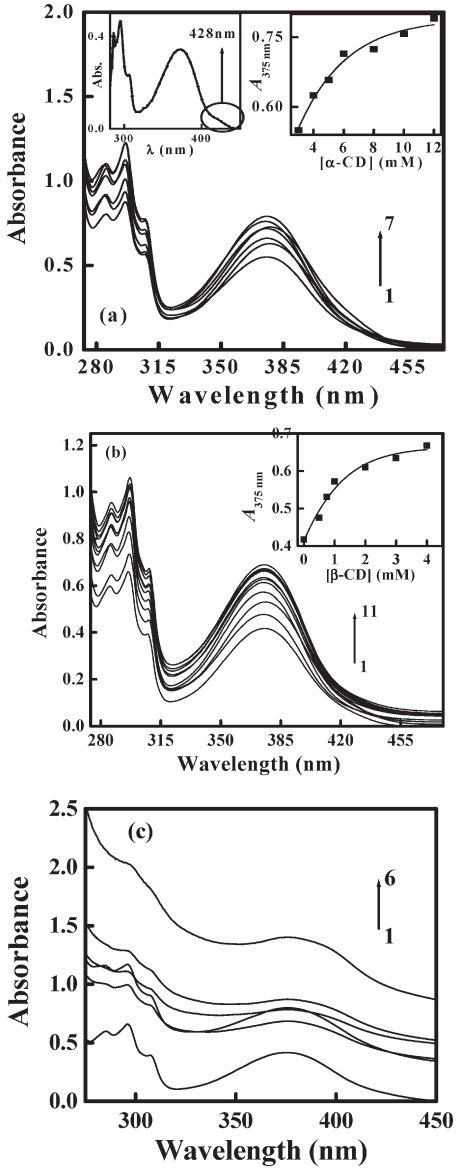

Figure 1. Absorption spectra of HN12 in presence in increasing concentration of (a) α-CD (Curves 1→7 correspond to [α-CD] = 3, 4, 5, 6, 8, 10, 12 mM), (b) β-CD (Curves 1→11 correspond to [β-CD] = 0.5, 0.75, 1, 2, 3, 4, 5, 6, 8, 10, 12 mM), and (c) γ-CD (Curves 1 → 6 correspond to [γ-CD] = 0.75, 2, 3, 4, 5, 6 mM). Insets show the variation of absorbance (at λ_{abs} = 375 nm) of HN12 as a function of CD concentration. The leftmost inset graph of Figure 1a shows the absorption spectrum of HN12 in pure aqueous solution to clearly present the band of hydrated cluster of HN12 at ~428 nm.

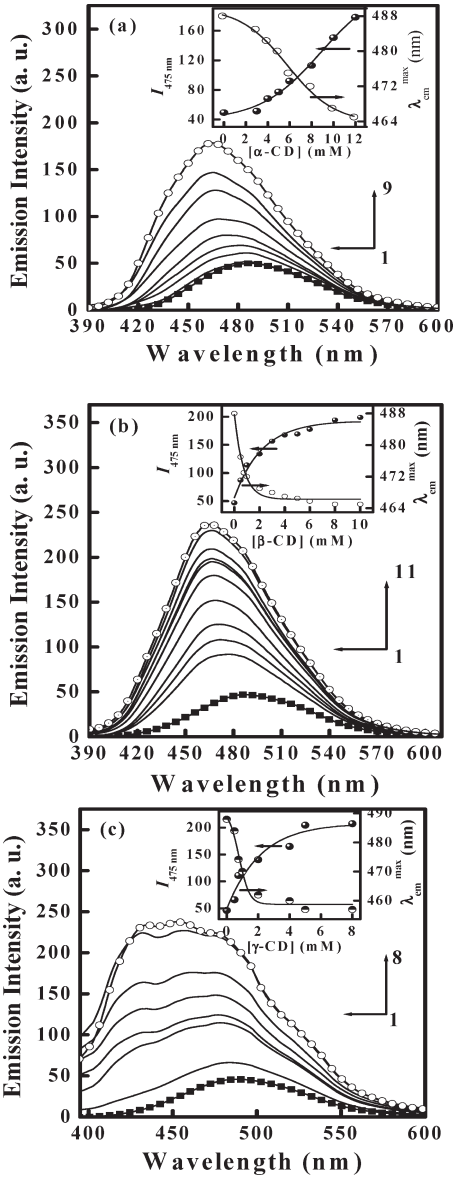

Figure 2. Emission spectra (λ_{ex} = 375 nm) of HN12 in the presence of increasing concentration of (a) α-CD (Curves 1 → 9 correspond to [α-CD] = 0, 3, 4, 5, 6, 8, 10, 11, 12 mM), (b) β-CD (Curves 1 → 11 correspond to [β-CD] = 0, 0.5, 0.75, 1, 2, 3, 4, 5, 6, 8, 10 mM), and (c) γ-CD (Curves 1 → 8 correspond to [γ-CD] = 0, 0.5, 0.75, 2, 4, 5, 6, 8 mM). Insets show the variation of emission intensity and λ^{em}_{max} of HN12 as a function of CD concentration.

the T*-form (Scheme 1) produced through an intrinsic proton exchange reaction in photoexcited HN12 and thus conversely the slower component is becoming responsible for the open form (II in Scheme 1). This observation advocates for the inherent ultrafast nature of the ESIPT reaction in HN12. At the same time, a major contribution from the T*-form seems consistent with the occurrence of ESIPT in HN12, since on the S_1-surface, the T*-form should be the more stable conformer than the E*-form.[34] Considering the ultrafast nature of the ESIPT process in HN12, the enhancement of the rate of ESIPT in CD can be excluded from being a probable reason of increment of the quantum yields of the tautomer emission of HN12; rather, the responsible factor is the retardation of the rate of radiationless transition due to the spatial and hydrophobic interaction with CDs. Roberts et al.[30] obtained similar results for inclusion complexes of 10-hydroxybenzo-[*h*]quinoline in β-CD and γ-CD, and they interpreted the results in a similar manner. However, they did not address another possibility that can be debated. Although ESIPT is a very fast process and has no intrinsic barrier, it depends upon the polarity of the solvent microenvironment. The solvent could play a crucial role in terms of introducing a "solvent-induced barrier"[7,38,39] to ESIPT reaction. The solvent-induced barrier to ESIPT originates from the interaction of the normal (**I**) and tautomer (**T**, Scheme 1) dipole with the polarization of the surrounding solvent and is determined by solvent dielectric properties.[7,38,39] In the solvophobic CD interior, the "solvent induced barrier" to ESIPT decreases, favoring enhancement of the rate of ESIPT, resulting

(38) Swinney, T. C.; Kelley, D. F. *J. Phys. Chem.* **1991**, *95*, 10369.
(39) Brucker, G. A.; Swinney, T. C.; Kelley, D. F. *J. Phys. Chem.* **1991**, *95*, 3190.

in enhanced tautomer emission in inclusion complexes as rapid ESIPT outweighs the effect of competing nonradiative processes for the depopulation of photoexcited closed conformer (Scheme 1).

It is noteworthy here that the solvent polarity/dielectric property may play a role in controlling the dynamics of ESIPT. It is well-established that the hydrogen bonding property of solvent molecules perturbs ESIPT through external H-bonding interaction with the solute molecule and retards the ESIPT rate. For example, the phototautomers of (hydroxyphenyl)benzazoles due to ESIPT have been demonstrated to be more efficiently produced in dry hydrocarbon solvents as compared to alcohols or water due to less (or absence of) competition between intra- and intermolecular H-bonding with the solvent molecules.[40,41] Thus, the most important and predominant factor that contributes to the enhancement of tautomer emission of HN12 in inclusion complexes of CDs seems to be the lower H-bonding interaction of CD interior rather than its less polar environment.

The excitation spectra (Figures 3) monitored at the corresponding emission maxima are found to reasonably match with the absorption spectra indicating that the emitting state has the same origin and a single type of equilibrium is present in the HN12:CD mixed system in the aqueous medium.[24,25]

3.3. Stoichiometric Ratio and Binding Strength between CDs and HN12. A quantitative estimate of the process of inclusion complex formation has been achieved on the basis of modified Benesi−Hildebrand plot[42] with a view toward evaluation of stoichiometry of the complex and binding constant (K_1) and free energy change (ΔG) of the process. Assuming 1:1 complexation between HN12 and CD, the equilibrium can be represented as

$$\mathrm{HN12} + \mathrm{CD} \rightleftharpoons \mathrm{HN12:CD} \tag{5}$$

and the corresponding equilibrium constant (K_1) is given as

$$K_1 = \frac{[\mathrm{HN12:CD}]}{[\mathrm{HN12}][\mathrm{CD}]} \tag{6}$$

where the terms within square brackets represent concentrations of the respective species.

A detailed discussion on Benesi−Hildebrand equation is avoided, since it is routine and is profusely available in the literature.[24−27,42] We thus start with the equation

$$\frac{1}{\Delta I} = \frac{1}{\Delta I_{\max}} + \frac{1}{K_1[\mathrm{CD}]\Delta I_{\max}} \tag{7}$$

where $\Delta I = I_t - I_0$ and $\Delta I_{\max} = I_\infty - I_0$ and I_0, I_t, and I_∞ are the emission intensities of HN12 in the absence of CD, at an intermediate concentration of CD, and at a concentration of complete interaction, respectively. By rearranging eq 7, the following form is obtained:

$$\frac{(I_\infty - I_0)}{(I_t - I_0)} = 1 + \frac{1}{K_1[\mathrm{CD}]} \tag{8}$$

Thus, in the case of a 1:1 complex, a plot of $(I_\infty - I_0)/(I_t - I_0)$ vs $[\mathrm{CD}]^{-1}$ should yield a straight line.

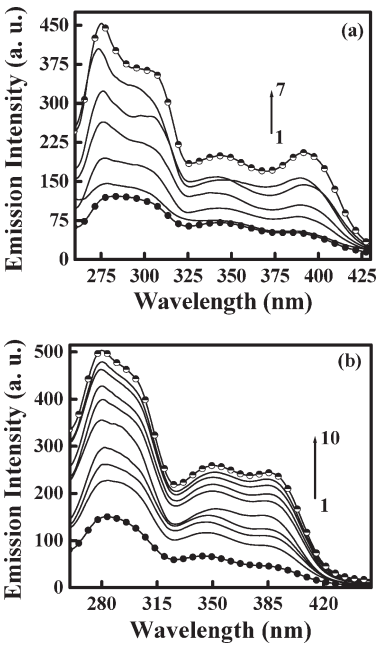

Figure 3. Fluorescence excitation spectra ($\lambda_{\mathrm{monitored}} = \lambda_{\mathrm{em}}$) of HN12 in the presence of increasing concentration of (a) α-CD (Curves 1→7 correspond to [α-CD] = 3, 4, 5, 6, 8, 10, 11 mM) and (b) β-CD (Curves 1→10 correspond to [β-CD] = 0.5, 0.75, 1, 2, 3, 4, 5, 6, 8, 10 mM).

Similarly, for 2:1 complex, the complexation equilibrium is presented as

$$\mathrm{HN12} + 2\mathrm{CD} \rightleftharpoons \mathrm{HN12:CD_2} \tag{9}$$

and the corresponding equilibrium constant is given as

$$K_2 = \frac{[\mathrm{HN12:CD_2}]}{[\mathrm{HN12}][\mathrm{CD}]^2} \tag{10}$$

and in terms of emission intensity of the probe, the expression takes the form

$$\frac{(I_\infty - I_0)}{(I_t - I_0)} = 1 + \frac{1}{K_2[\mathrm{CD}]^2} \tag{11}$$

i.e., the formation of a 2:1 complex will be revealed through a linear regression of $(I_\infty - I_0)/(I_t - I_0)$ vs $[\mathrm{CD}]^{-2}$ plot.

From the analysis of fluorescence data, the modified Benesi−Hildebrand plot is found to reveal a 1:1 association for HN12:β-CD (Figure 4b) and HN12:γ-CD (Figure 4c) inclusion complexes. β- and γ-CDs have different cavity diameters (i.e., 7.8 and 9.5 Å, respectively[43]), and the length of the molecule is predicted to be $a = 4.57$ Å calculated at DFT/B3LYP/6-31G** level of theory. Thus, a 1:2 HN12:γ-CD complex seems plausible considering cavity diameter, but both β- and γ-CDs have similar cavity lengths (~0.78 Å),[43] which may restrict the accommodation of two HN12 molecules into one β- or γ-CD cavity.

The situation is, however, different in the case of α-CD in which a similar analysis of the fluorescence data is found to suit to a 1:2 association for HN12:α-CD complex (Figure 4a). These results are also found consistent considering the optimized length of HN12 and the cavity diameter of α-CD, which is ~4.5 Å.[26,43]

(40) Elsaesser, T.; Schmetzer, B. *Chem. Phys. Lett.* **1987**, *140*, 293.
(41) Potter, C. A. S.; Brown, R. G. *Chem. Phys. Lett.* **1988**, *153*, 7.
(42) Carter, D. C.; Ho, J. X. *Protein Chem.* **1994**, *45*, 153.
(43) Li, S.; Purdy, W. C. *Chem. Rev.* **1992**, *92*, 1457 and references therein.

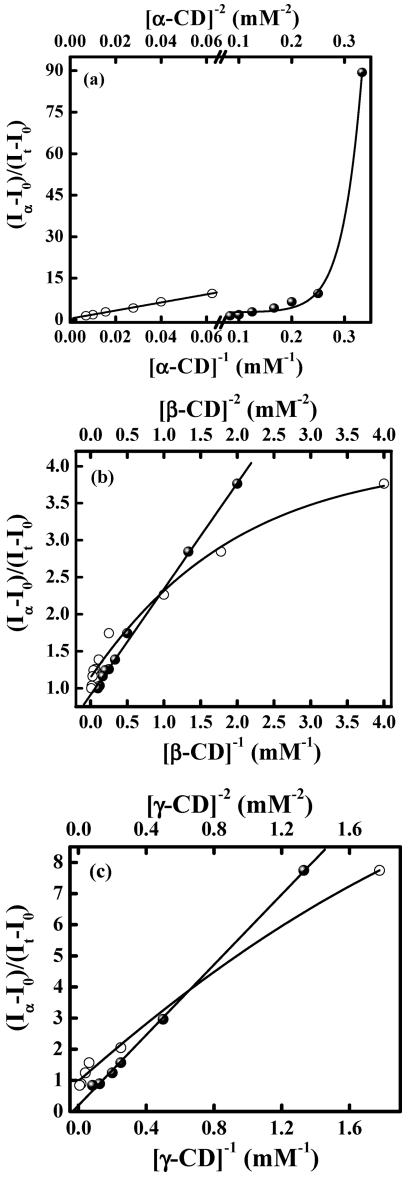

Figure 4. $(I_\infty - I_0)/(I_t - I_0)$ vs $[CD]^{-1}$ plot using fluorescence data for complexation of HN12 with (a) α-CD, (b) *β*-CD, and (c) *γ*-CD assuming 1:1 (solid circle) and 1:2 (open circle) stoichiometries.

It is thus reasonable to assume that complex formation between HN12 and α-CD requires the involvement of two α-CD molecules (Scheme 2). Also, in case of α-CD, changes in the absorption/emission spectra came into operation only above [α-CD] = 3 mM (as already mentioned in section 2.2) seem to stand by the conclusion that a 1:2 association has been operative in the case of HN12:α-CD complexation.

The formation constant values (K_1) obtained from the slopes of the respective linear regressions (Figure 4) and the calculated free energy changes for complexation reaction ($\Delta G = -RT \ln K_1$) are summarized in Table 1. A remarkably high association constant (K_2) for the 1:2 HN12:α-CD complexation signifies a compact packing of the probe within the cavity space of two α-CDs coming from opposite directions (Scheme 2). The estimated formation constant values comply well with the normal range of magnitude reported earlier for such type of complexation.[24−27,30] However, it is worth keeping in mind that the Benesi−Hildebrand plot delivers greater emphasis on lower concentration values than on higher ones. Thus, the slope of the line is more sensitive to ordinate values of the point with the smallest concentration.[30,31,42]

Scheme 2. (a) Optimized Structure of HN12 (DFT/B3LYP/6-31G) and Probable Structure of Inclusion Complexes with (b) *β*- (or *γ*-) Cyclodextrin (1:1 stoichiometry) and (c) α-Cyclodextrin (1:2 stoichiometry)**

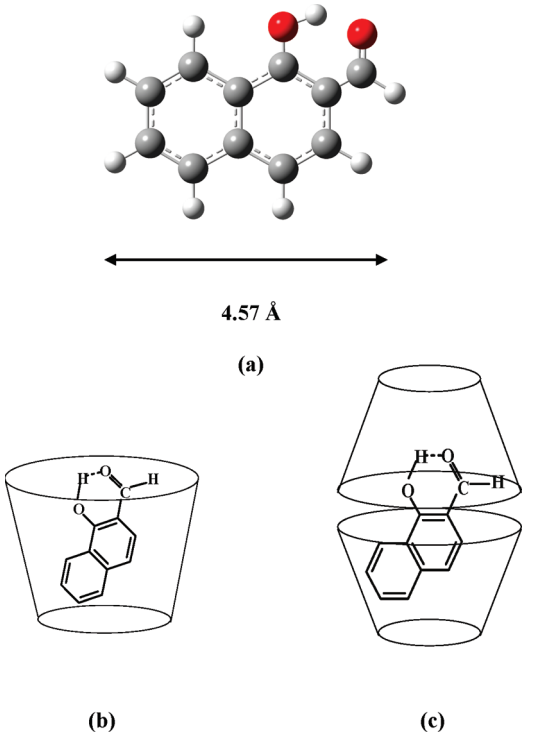

Table 1. Formation Constants (K_1/K_2) and Free-Energy Changes (ΔG) for Interaction of HN12 with Cyclodextrins and Micelles in Aqueous Medium at Ambient Temperature (27 °C)

host	guest	host:guest	K_1/K_2 (M^{-1}/M^{-2})	$-\Delta G$ (kJ mol^{-1})	R^a
α-CD	HN12	2:1	$6.86 \times 10^3 \pm 0.12$	22.03	0.99168
β-CD	HN12	1:1	699.21 ± 9.91	16.34	0.99808
γ-CD	HN12	1:1	177.00 ± 4.38	12.91	0.98959
SDS	HN12	--;	$0.37 \times 10^5 \pm 2.22$	26.24	0.99800
TW-20	HN12	--;	$31.14 \times 10^5 \pm 1.50$	38.68	0.98185

[a] R is the correlation factor of the respective linearized Benesi−Hildebrand plots showing the excellence of the linear fit.

3.4. Effect of Variation of pH. Experimental findings presented in the foregoing sections evidence the complex formation between HN12 and cyclodextrin, and the stoichiometry of the complexes with different CDs are also determined by employing Benesi−Hildebrand relation. It is thus pertinent at this point to have an idea about the orientation of the probe molecule in the CD interior. For this purpose, effects of pH on the absorption and emission spectra in the presence of CD have been recorded and compared with the results obtained in the absence of CD.

It is reported that HN12 generates anion absorption band at ~400 nm for conformer **I** together with an absorption band due to similar type of anion formation of the unsolvated open conformer (~325 nm) in the presence of base NaOH. On the emission profile, a blue shift of the tautomer emission was observed upon increasing the pH of the medium, and this band was assigned to the anion (λ_{em} = ~460 nm) of the molecule formed as a result of abstraction of the hydroxyl proton.[34]

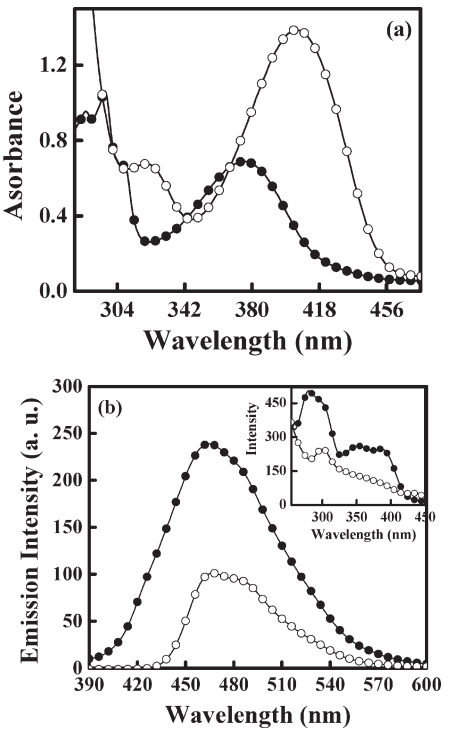

Figure 5. Effect of addition of base (aqueous NaOH solution) on (a) absorption spectra and (b) emission spectra ($\lambda_{ex} = 375$ nm) (inset: excitation spectra) of HN12 in the presence of 10 mM β-CD (-●- in the absence of OH^- and -○- in the presence of OH^-).

An increment of pH of the medium in the presence of β-CD is found to yield similar results, i.e., generation of two new absorption bands at ~325 nm and ~400 nm, which are due to the anion of the unsolvated open conformer (**II**, Scheme 1) and the closed conformer (**I**, Scheme 1), respectively (Figure 5a), indicating that during encapsulation of HN12 within β-CD interior the orientation of the molecule is such that the −OH and −CHO functional moieties are still exposed outside the CD cavity and hence accessible to OH^- so as to produce qualitatively similar observations to that in absence of β-CD. Similar observations for the HN12:γ-CD complex suggest a similar type of orientation inside γ-CD cavity also (figure not given). A similar experiment on the HN12:α-CD complex was found to yield no noticeable spectral modifications as can be complemented from the estimation of a 1:2 stoichiometry in the present case, which subsequently screens the fluorophore from external perturbations (external agent like OH^- ion). However, it is ethical to mention that during base treatment on the HN12:α-CD complex only a low concentration of the base (NaOH) was added, as for otherwise it led to the appearance of turbidity in the medium, which subsequently accompanied a considerable deformation of the shape of the absorption spectra.

On the emission profile, however, the fruitfulness of pH variation experiments in aqueous CD medium (Figure 5b) in furnishing information regarding the orientation of the probe inside CD cavity has been crumpled by the overlying location of the emission maxima of HN12:CD complex ($\lambda_{em} \sim 460$ nm) and anion of HN12 ($\lambda_{em} \sim 460$ nm).

3.5. HN12 in Micellar Media. Surfactants, through formation of micelles, can enormously modify the photophysics/photochemistry of a compound by providing an environment of varied micropolarity and rigidity inside the heterogeneous micellar microenvironments compared to that in bulk homogeneous fluid. The organized micellar media can then serve to protect the compound from external perturbations in solution; also, entrapment within micellar cavity may result in appreciable modulation in rates of various physical and/or chemical processes.

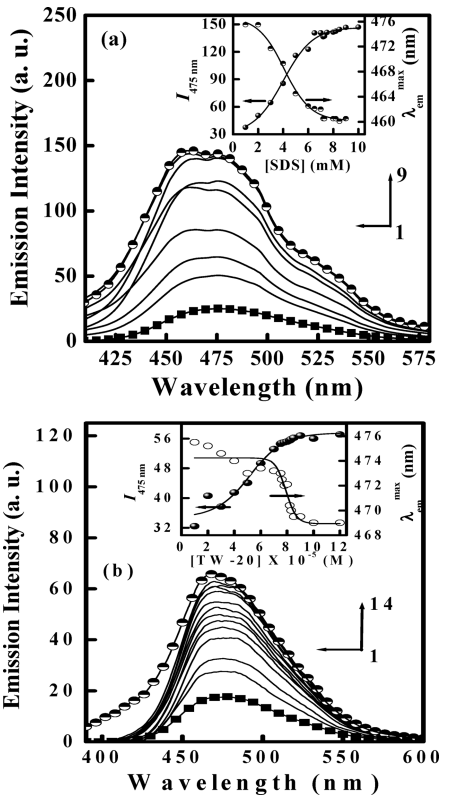

Figure 6. Emission spectra ($\lambda_{ex} = 375$ nm) of HN12 in the presence of increasing concentration of (a) SDS (Curves 1→9 correspond to [SDS] = 0, 2, 3, 4, 5, 6, 6.5, 7, 8.2 mM) and (b) TW-20 (Curves 1→14 correspond to [TW-20] = 0, 10, 20, 30, 50, 60, 70, 80, 90, 100, 110, 120, 130, 140 μM) surfactant. Insets show the variation of emission intensity (at $\lambda_{em} = 475$ nm) and λ^{em}_{max} of HN12 against surfactant concentration.

Addition of both ionic (sodium dodecyl sulfate, SDS) and nonionic (Tween 20, TW-20) surfactant, individually, to an aqueous solution of HN12 is found to associate an increment in absorbance with no significant shift of the absorption maxima (graph not given). Such changes in the absorption spectra of HN12 in the presence of surfactants may serve as an indication of the interaction between the two concerned parties. Changes in the emission spectral properties of HN12 in micellar media follow a similar trend as that in the case of incorporation of HN12 in CD nanocavity. As seen in Figure 6a,b, gradual addition of SDS and TW-20 to an aqueous solution of HN12 accompanies an enhancement of fluorescence intensity along with a shift of the emission maxima toward the blue. Zaitsev et al. observed a similar dependence of fluorescence quantum yield of probe acridinium ion on SDS concentration.[44] According to them, this dependence of quantum yield on SDS concentration is the result of static quenching (aggregation) of fluorescent probe at very low concentration of SDS (below CMC). Once SDS concentration exceeds CMC value, fluorescence intensity increases due to ground-state dissociation of the aggregates and concentration self-quenching of the probe follows to the dynamic mechanism, and its fluorescence lifetime and quantum yield gradually rises with surfactant concentration. Consistent with the

(44) Zaitsev, A. K.; Zaitsev, N. K.; Pavlov, A. A.; Kuzmin, M. G. *Russ. Chem. Phys.* **1985**, *4*, 182.

above-mentioned case of acridinium ions, the intensity variation of HN12 in the presence of surfactants can also be ascribed to the formation of premicellar aggregates between HN12 and surfactant molecules before CMC. However, the initial rapid enhancement of intensity of the PT emission band with surfactant concentration is attributable to the increment of quantum yield with increasing hydrophobicity of the microenvironment surrounding the probe, which leads to more efficient solubilization of the probe in the medium due its neutral, nonpolar character. In the bulk aqueous phase, the possibility of radiationless deactivation is operative through enormous intermolecular hydrogen bonding, and hence, the intensity of the PT band is reduced, e.g., in the case of dyes, stronger hydrogen bonding solvents have been found to cause a larger rate of singlet to triplet intersystem crossing.[45] Such funneling out energy via the agency of nonradiative decay channels decreases with increase of surfactant concentration leading to subsequent emission intensity enhancement. For the region above CMC, modifications to spectral properties of HN12 are minimized upon further addition of the surfactants as reflected by near-constancy in emission intensity. The probe molecules in this region remain solubilized in micelles.

The insets of Figure 6 reveal the variation of emission intensity and emission maxima as a function of surfactant concentration allowing one to have an idea about the CMC of the individual systems, which are consistent with literature values.[13,26]

3.6. Estimation of HN12−Micelle Binding Interaction. The caliber of HN12 to serve as a molecular reporter for investigation of micellar microenvironments is directly dependent upon its binding ability. In order to derive a quantitative estimate of the binding interaction between HN12 and micellar media in terms of binding constant (K_1) and free energy change (ΔG), we have followed the method described by Almgren et al.[46] According to this method, the binding phenomenon between the fluorophore and micellar medium is described by the following expression:

$$\frac{I_\infty - I_0}{I_t - I_0} = 1 + \frac{1}{K_1[\mathrm{M}]} \qquad (12)$$

in which I_0, I_t, and I_∞ are the emission intensities of the probe, respectively, in the absence of surfactant, at an intermediate concentration of surfactant, and at a condition of saturation. The micellar concentration [M] is given as

$$[\mathrm{M}] = \frac{[\mathrm{S}] - \mathrm{CMC}}{N_{\mathrm{agg}}}$$

in which [S] represents the surfactant concentration and N_{agg} is the aggregation number of the micellar system. The values of N_{agg} for SDS[47] and TW-20[48] have been taken from literature. Figure 7 reveals linear regression for $(I_\infty - I_0)/(I_t - I_0)$ vs $[\mathrm{M}]^{-1}$ plot according to eq 12. The estimated binding constant (K_1) and free energy change values are collected in Table 1 and are

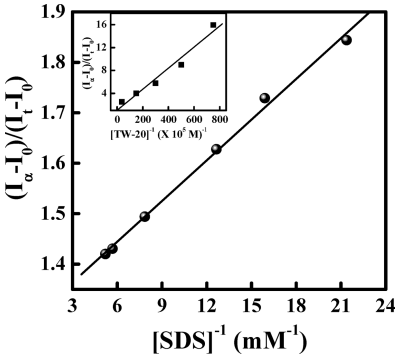

Figure 7. Plot of $(I_\infty - I_0)/(I_t - I_0)$ vs $[\mathrm{SDS}]^{-1}$. The corresponding plot for TW-20 is given in the inset since the scales are different.

found to comply with some other similar reports available in the literature.[24−27,30,49]

Relatively weaker binding between HN12 and the ionic micelle SDS seems to stem from the fact that all the heteroatoms of the probe are endowed with partial negative charge (as found from DFT/B3LYP/6-31G** theoretical calculation[34]), which are expected to experience a repulsive impulse from the negatively charged SDS micellar units.[49]

3.7. Action of Urea on Micelle-Bound Probe. Recent time has witnessed an upcoming urge to investigate the action of urea on micellar solutions with the aim of gaining better insight into the mode of action of urea in complex biological systems implementing micelles as simpler models. The denaturing action of urea is generally explained on the basis of two mechanisms. One is an indirect mechanism in which urea is believed to act only at the level of the solvent, altering the structure of water in a way that facilitates the dissolution of hydrophobic probes, i.e., by invoking the capacity of urea as "water structure breaker" and thereby decreasing the free energy required for cavity formation.[50] The other is a direct mechanism in which urea participates in the solvation of hydrophobic species by replacing some water molecules in the hydration shell of the solute. However, the issue of superiority of one mechanism over the other is still a matter of open debate. Therefore, in the present work we have attempted to address the problem by elucidating the action of urea on surfactants (SDS and TW-20) taking HN12 as the molecular reporter (Figure 8).

Addition of urea to the micelle-bound probe is found to induce decrement of intensity with concomitant red shift of the emission maxima, suggesting that the treatment with urea results in expulsion of the probe molecules from the microheterogeneous environment to the bulk aqueous phase. However, the observations in SDS medium are not very different from that in TW-20 medium. In the presence of 8 M urea in SDS-bound HN12, the fluorescence emission intensity of the fluorophore (for the same concentration of HN12 with all other experimental conditions conserved) is still higher than that in pure aqueous medium (Figure 6a) and the emission maxima is only insignificantly shifted, whereas in TW-20-bound probe, the emission maxima and emission intensity of HN12 closely correspond to those in the aqueous phase (Figure 6b). Such a differential response of HN12 under the same experimental conditions is a direct manifestation of the fact that urea is able to expel HN12 more efficiently from TW-20 micellar units compared to the SDS micellar system. This can be rationalized in terms of the extent of water penetration into the respective micellar systems. It is believed that the ability of

(45) Das, R.; Guha, D.; Mitra, S.; Kar, S.; Lahiri, S.; Mukherjee, S. *J. Phys. Chem. A* **1997**, *101*, 4042.
(46) Almgren, M.; Grieser, F.; Thomas, J. K. *J. Am. Chem. Soc.* **1979**, *101*, 279.
(47) Weidemaier, K.; Tavernier, H. L.; Fayer, M. D. *J. Phys. Chem. B* **1997**, *101*, 9352.
(48) Lee, M. S.; Park, S. S.; Lee, G. D.; Ju, C. S.; Hong, S. S. *Catal. Today* **2005**, *101*, 283.
(49) (a) Mallick, A.; Haldar, B.; Maiti, S.; Chattopadhyay, N. *J. Colloid Interface Sci.* **2004**, *278*, 215. (b) Chakrabarty, A.; Das, P.; Mallick, A.; Chattopadhyay, N. *J. Phys. Chem. B* **2008**, *112*, 3684.
(50) Albuin, E.; Lissi, E. *South. Braz. J. Chem.* **1994**, *2*, 71.

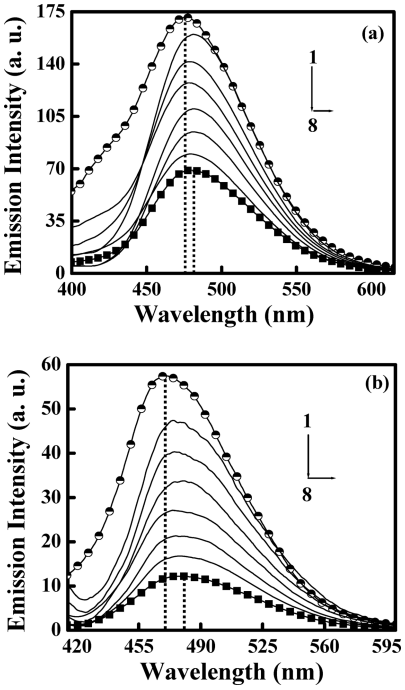

Figure 8. Emission spectra (λ_{ex} = 375 nm) of micelle-bound HN12 in the presence of increasing urea concentration. (a) [SDS] = 10 mM and curves 1 → 8 correspond to 0, 1, 2, 3, 4, 5, 7, 8 M urea; (b) [TW-20] = 100 μM and curves 1→8 correspond to 0, 1, 2, 3, 5, 6, 7, 8 M urea.

water molecules to penetrate into the micelles depends on the compactness of the micellar units,[51] e.g., the extent of water penetration into micelles with compact head groups like SDS is considerably negligible compared to those with larger head groups such as TW-20. Thus, urea removes the solvent molecules adjacent to the microheterogeneous environments when the consequent destabilization of the environment results in desolvation of the guest molecules and expels it to the bulk aqueous phase. Such a proposition is consistent with an earlier report by Mallick et al.[49]

3.8. Wavelength-Sensitive Fluorescence Behavior of HN12 in Different Organized Media. Red edge excitation shift (REES)[52−55] is a well-known phenomenon which provides a more vivid picture of the surrounding atmosphere of the probe while emitting from an excited state, particularly when in an organized medium. REES measurement is exploited extensively in biochemical and biophysical research for its excellent ability to furnish important information regarding direct monitoring of solvation dynamics within organized media.[13,15,56] An excellent review on this topic by Demchenko is available in the literature.[57a] Here, we have observed the dependence of emission maxima on the excitation wavelength (REES) in HN12 when it is present in organized media provided by the CDs and micellar cavities. Some of the earlier explanations of REES involve emission from more

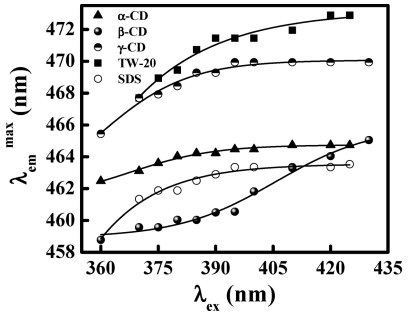

Figure 9. Variation of emission maxima of the CD/micelle-bound probe (HN12) as a function of excitation wavelength. [CD/SDS] = 10 mM and [TW-20] = 100 μM.

than one electronic state or from different conformers of the molecule. It is now fairly well understood that REES in organized assemblies arises primarily out of the spatial heterogeneity of these assemblies, which consist of hydrophobic and hydrophilic pockets that allow multiple solvation sites and contribute to inhomogeneous broadening of the absorption spectra.[56,57] Such broadening allows the provision of site photoselection by excitation and emission quanta.

The excitation wavelength dependence can, however, arise when there exists an ensemble of molecules in the ground state, which differ in their solvation sites and, hence, their energies. This inhomogeneity is not unlikely with a view to the difference in interaction energies between the probe molecule HN12 and different organized media, i.e., CDs and micellar media. However, the presence of an ensemble of energetically different molecules in the ground state alone does not guarantee the occurrence of REES due to rapid relaxation of the excited state,[57] such as the solvation of the fluorescent state or the energy transfer between the energetically different excited states or conformers of the molecule, might result in emission from the lowest-energy state irrespective of the excitation. It is only when a system allows selective excitation of the energetically different species and the relaxation of the fluorescent state is slow and hence incomplete that REES can be expected. In organized media, the solvent dipoles experience greater restriction on their mobility and thus take a longer time to reorient themselves around the excited fluorophore, whereas in pure solvent, emission always occurs from the solvent relaxed state of the excited fluorophore. Thus, the phenomenon of REES provides a more vivid picture of the surrounding atmosphere of the fluorophore while emitting from the excited state.

However, for the occurrence of REES some requirements need to be satisfied, such as the following:[57] (i) The molecule should be polar with dipole moment higher in the excited state than that in the ground state. In fact, the extent of inhomogeneous broadening of the absorption spectra allowing the provision of site photoselection of energetically different species is dependent on the change of dipole moment ($\Delta\mu$) upon photoexcitation, (ii) The solvent molecules around the fluorophore must be polar and the solvent reorientation time ($\langle\tau_{solvent}\rangle$) should be equal to or longer than the fluorescence lifetime (τ_f) of the fluorophore so that unrelaxed fluorescence can give rise to excitation-wavelength-dependent emission behavior.

Figure 9 displays the variation of emission maxima as a function of excitation wavelength in different organized media of CDs and micelles, under similar experimental conditions and for the same change of excitation wavelength. A maximum REES value of 6.35 nm is obtained in the case of β-CD, while the trend is β-CD > TW-20 > γ-CD ≈ SDS > α-CD. Now, since the lifetime

(51) Muller, N. In *Reaction Kinetics in Micelles*, Cordes, E. A., Ed.; Plenum: New York, 1973.
(52) Galley, W. C.; Purkey, R. M. *Proc. Natl. Acad. Sci. U.S.A.* **1970**, *67*, 1116.
(53) Rubinov, A. N.; Tomin, V. I. *Opt. Spektr.* **1970**, *29*, 1082.
(54) (a) Weber, G.; Shinitzky, M. *Proc. Natl. Acad. Sci. U.S.A.* **1970**, *65*, 823. (b) Weber, G. *J. Biochem.* **1960**, *75*, 335.
(55) Lakowicz, J. R. *Principles of Fluorescence Spectroscopy*; Plenum: New York, 1999.
(56) Mukherjee, S.; Chattopadhyay, A. *Langmuir* **2005**, *21*, 287.
(57) (a) Demchenko, A. P. *Luminesc.* **2002**, *17*, 19. (b) Demchenko, A. P.; Ladokhin, A. S. *Eur. Biophys. J.* **1988**, *15*, 369. (c) Samanta, A. *J. Phys. Chem. B* **2006**, *110*, 13704. (d) Mandal, P. K.; Sarkar, M.; Samanta, A. *J. Phys. Chem. A* **2004**, *108*, 9048.

Table 2. Fluorescence Lifetime, Quantum Yield, and Radiative and Non-Radiative Rate Constants of HN12 in Different Organized Media of CDs and Micelles

environment	a_1	a_2	a_3	τ_1 (ns)	τ_2 (ns)	τ_3 (ns)	$\langle\tau_f\rangle$ (ns)	χ^2	quantum yield (Φ_f)[a]	$k_r \times 10^{11}$ (s^{-1})	$k_{nr} \times 10^9$(s^{-1})
water	0.91	0.09	--	0.087 ± 0.04	0.588 ± 0.02	--	0.2877	1.50	0.668	2.3218	3.4526
α-CD	0.1143	0.0912	0.7943	0.9900 ± 0.02	5.1294 ± 0.03	0.0796 ± 0.02	3.9068	1.00	2.54	0.6513	0.2494
β-CD	0.3152	0.6457	0.0390	1.0073 ± 0.02	0.1424 ± 0.06	4.0021 ± 0.03	1.6935	1.09	3.52	2.0783	0.5697
SDS	0.0524	0.0049	0.9427	0.6732 ± 0.03	2.7943 ± 0.10	0.06792 ± 0.11	0.5877	0.99	2.34	1.958	0.8155
TW-20	0.1967	0.0095	0.7536	1.2033 ± 0.1	3.69025 ± 0.07	0.10766 ± 0.04	1.19747	1.11	1.93	3.289	1.6686

[a] Quantum yields are $\times 10^{-2}$ order.

measurements confirm that encapsulation of HN12 in CDs or micellar interior associates an increase of fluorescence lifetime compared to that in pure aqueous solution (Table 2) and the mean (average) lifetime values are quite high, it seems reasonable to propose that the observed REES in the studied organized media is not due to fluorescence from an unsolvated (or partially solvated, and hence incompletely relaxed) state; rather fluorescence occurs from fully solvated state in these systems since the fluorescence lifetime values are longer than (or comparable to) the solvent relaxation time. Rather, some other sort of interactions seems to play the vital role in creating a distribution of energetically different molecules in the ground state that allows their photoselection. This idea goes in line with other studied systems for REES in different environments.[55−58] From the structural point of view, the unique nature of HN12 is quite interesting in the sense that it happens to contain two functional groups capable of forming hydrogen bond, but the −OH group can enter into hydrogen bonding primarily by donating the hydrogen atom, whereas the participation of −CHO group in hydrogen bonding will accompany its function as hydrogen acceptor. That hydrogen bonding interactions in different environments lead to further complication in the photophysics of HN12 is evident from its photophysical studies.[34] Thus, it seems reasonable that different types of hydrogen bonding interaction and their perturbations or modifications to different extents under different complex environments provided by CD nanocavities or micellar media might play a role in producing ground-state inhomogeneity, thereby allowing initial photoselection. However, it is not easy to be very particular about the reason stated above given the inherently complex nature of hydrogen bonding interaction and also the complexity provided by CD and micellar cavities.

3.9. Time-Resolved Study: Radiative and Nonradiative Rates. The changes in the fluorescence lifetime help to provide an insight into the modulations of radiative and nonradiative deactivation channels brought about by encapsulation of the probe.[7,13,26,27] It is seen that the fluorescence decays of HN12 in all of the environments studied, including pure water, are far from single exponential. In water, the decay is found to fit in biexponential function, whereas in CDs and micelles, the decay patterns are even more complicated and are found to be triexponential. Figure 10 depicts the fluorescence decay profile of the PT emission of HN12 (monitored at 460 nm and $\lambda_{ex} = 375$ nm) in presence of CDs and micelles. However, given the complex and multiexponential nature of the decay patterns, it is really difficult to specify the particular values of the rate constants in such heterogeneous systems. Thus, in order to realize the effect of encapsulation of the fluorophore on the overall radiative and nonradiative decay rates, we preferred to use the mean fluorescence lifetime as defined by eq 1 instead of placing too much emphasis on individual components of the multiexponential decays. The calculated values of the

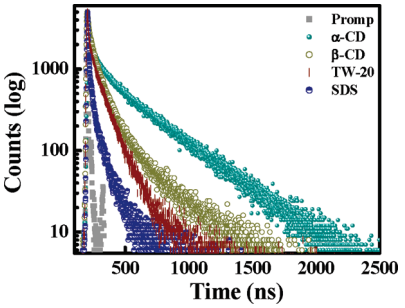

Figure 10. Typical fluorescence decay profile of HN12 in different confined environments ([CD/SDS] = 10 mM and [TW-20] = 100 μM; $\lambda_{ex} = 375$ nm and $\lambda_{monitored} = 460$ nm).

average lifetimes are given in Table 2. The effect of the confined environment in all the cases is found to be in enhancement of average fluorescence lifetime compared to that in bulk aqueous phase. This is entrusted on reduction of intermolecular hydrogen bond assisted radiationless decay channels present in bulk aqueous phase compared to the entrapment of HN12 inside hydrophobic core of the organized media.

Now, from the calculated fluorescence quantum yield (Φ_f) and average fluorescence lifetimes ($\langle\tau_f\rangle$) (Table 2), we have calculated the radiative and nonradiative decay rate constants for the overall deactivation process of the excited probe using the following equations

$$k_r = \frac{\Phi_f}{\langle\tau_f\rangle} \quad \text{and} \quad \frac{1}{\langle\tau_f\rangle} = k_r + k_{nr}$$

where k_r and k_{nr}, respectively, indicate the radiative and nonradiative rate constants. From Table 2, it is evident that the nonradiative rate constant (k_{nr}) is higher in pure aqueous medium compared to that in the restricted media. Thus, an enhancement in the radiative lifetime ($\langle\tau_f\rangle$) and fluorescence intensity of HN12 in the organized media can be realized in connection with reduction in the radiationless decay channels in these environments.

3.10. Steady-State Fluorescence Anisotropy Measurement. Fluorescence anisotropy is a property that depends on the rotational diffusion of the fluorophore and is a reflection of the degree of restriction imposed on the dynamic properties of the fluorophore by its microenvironment. The increase in the anisotropy value is a direct manifestation of the increased rigidity of the local environment of the probe.[26,27,55] Figure 11 displays the variation of fluorescence anisotropy (r) of HN12 with increasing concentration of cyclodextrin and surfactants. In the case of β-CD solution, the trend of variation of anisotropy is quite usual and follows the same trend as that of emission intensity with increasing concentration of β-CD. The increasing restriction imposed on the rotational motions of the fluorophore as a function of [β-CD] is clearly reproduced by the variation of

(58) Gratzel, M.; Thomas, J. K. In *Modern Fluorescence Spectroscopy*, Wehry, E. L., Ed.; Plenum Press: New York, 1976; Vol. *2*.

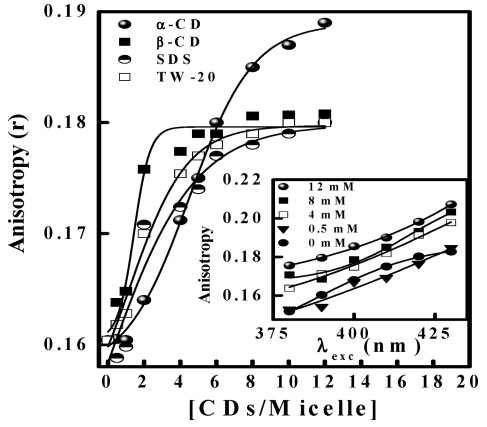

Figure 11. Variation of steady-state fluorescence anisotropy with increasing concentration of CDs/micelles (concentration of CDs and SDS in $\times 10^{-3}$ M order; concentration of TW-20 in $\times 10^{-5}$ M order; $\lambda_{ex} = 375$ nm and $\lambda_{em} = 460$ nm). Inset shows the variation of steady-state anisotropy values at definite concentrations of β-CD (indicated on the graph) plotted as a function of excitation wavelength.

anisotropy values. Similar results are obtained with micellar environments of SDS and TW-20. However, in case of α-CD, up to ~3 mM of α-CD concentration, anisotropy is practically independent of α-CD concentration and resembles the value obtained in bulk aqueous medium. This may well be an indication of the absence of α-CD:HN12 complexation. With further increase of [α-CD], the anisotropy increases steeply and finally attains the plateau at ~5 mM α-CD. This observation follows very well the results of emission spectral changes of HN12 in presence of α-CD (Figure 2a and section 2.2) and further reinforces the phenomenon of inclusion of HN12 in cavity of α-CD. Again, beyond CD concentration of 5 mM, the anisotropy increment for HN12 is found to surpass that for β-CD, a corroboration of the results of fluorescence lifetime measurements (Figure 10 and Table 2), i.e., formation of a 2:1 complex with α-CD is necessary to impart a greater degree of restriction on the rotational motions of HN12 as against the case of 1:1 complexation with β-CD. A direct manifestation of this is figured out in the trend of variation of anisotropy as a function of CD concentration.

In order to ensure that the observed changes in the anisotropy values of HN12 in the restricted environments are not due to any change in the lifetime, the apparent (average) rotational correlation times (τ_c) were calculated from Perrin's equation[26,55] at the saturation level.

$$\tau_c = \frac{\langle \tau_f \rangle r}{r_0 - r}$$

in which r_0, r, and $\langle \tau_f \rangle$ are the fundamental anisotropy for the complexed molecule, steady-state anisotropy, and mean fluorescence lifetime, respectively. Although ideally Perrin's equation is not applicable in a microheterogeneous environment, it can be used to a good degree of approximation considering the mean fluorescence lifetime of the system. Using the above equation, we have determined the τ_c values in the confined environments, (taking $r_0 = 0.38$).[26,55] The τ_c value is found to increase appreciably as the concentration of the encapsulated complex (HN12:CD/micelle) increases with addition of CD/micelle. A significant increase in the τ_c values in all the confined environments establishes that the observed changes in the anisotropy value were not due to lifetime-induced phenomena and seems to support our previous prediction that an increased restriction to the rotational motions experienced by the probe is responsible for increase in anisotropy values.

In addition, a more or less linear increase in the anisotropy value as a function of the excitation wavelength is observed for HN12 in all the restricted environments. Inset of Figure 11 shows the trend for different concentrations of β-CD (similar results are also obtained in other restricted media; the graphs are not shown). This effect is attributed to the slow rate of solvent reorientation around the fluorophore in the excited state in organized media and hints toward location of the probe in motionally restricted environments.[13,55−58]

4. Conclusion

A comparative study on the modulation of ESIPT reaction of HN12 in different supramolecular assemblies provided by cyclodextrins and ionic (SDS) and nonionic (TW-20) micelles has been explored by steady-state and time-resolved fluorescence and fluorescence anisotropy techniques. The experimental findings divulge the conjugate effect of polarity and rigidity of cyclodextrin nanocavities and micellar environments on the photophysics of HN12. Benesi−Hildebrand plot reveals the formation of 2:1, 1:1, and 1:1 inclusion complexes with α-, β-, and γ-cyclodextrins, respectively. Interestingly, the formation of a 2:1 (host:guest) stoichiometry with α-CD (host) necessitating the impartation of greater degree of motional restriction to the molecular skeleton of the guest HN12 is further reinforced from enhanced fluorescence lifetime and anisotropy values, and also complemented from a remarkably high magnitude of formation constant (K_1). The enhancement in absorbance and emission intensity of HN12 in CDs/micellar environments has been linked to the provision of a hydrophobic and more confined environment provided by the organized media resulting in retardation of radiationless decay channels, and this proposition is thoroughly supported by the time-resolved data. REES and steady-state anisotropy measurements afford additional support in favor of interaction between HN12 and CD/micelle. This work also demonstrates the differential effect of urea on the two micellar systems. The observed enhanced and spectral-shifted ESIPT emission of HN12 could have indications toward future applications in improving the characteristics of the probe as a promising agent in radiation-hard scintillators. Further, the ability of HN12 to depict changes in the microenvironments of cyclodextrins and micelles advocates its potential applicability as a molecular reporter for these media.

Acknowledgment. B. K. P. and A. S. acknowledge CSIR, New Delhi, India for Junior Research Fellowship. The authors like to convey their special thanks to Prof. T. Ganguly of Indian Association for the Cultivation of Science, Jadavpur, India, for fluorescence lifetime measurements. This work was supported by CSIR, India (Project no. 01(2161)07/EMR-II), DST, India (Project no. SR/S1/PC/26/2008) and CRNN, CU.